

Biomedical Research and Reviews

Perfusion and Oxygenation Changes after Isolated Limb Perfusion with TNF - α in Lower Limb Sarcoma: A Case Report

Katerina Nikiforaki^{1,2*}
Georgios C. Manikis^{1,2}
Maria Venianaki^{1,3}
Eleftherios Kontopodis^{1,2}
Eleni Lagoudaki⁴
Thomas G. Maris²
Kostas Marias^{1,5}
Eelco de Bree⁶
Apostolos Karantanas^{1,2}

¹Computational BioMedicine Laboratory (CBML), Foundation for Research & Technology, Greece

²Department of Radiology, School of Medicine, University of Crete, Greece

³Image Analysis Research Unit, IMT School for Advanced Studies Lucca, Italy

⁴Department of Pathology, University Hospital of Crete, Greece

⁵Technological Educational Institute of Crete, Department of Informatics Engineering, Greece

⁶Department of Surgical Oncology, School of Medicine, University of Crete, Greece

Abstract

Tumor necrosis factor alpha (TNF- α) is known to cause selective destruction of tumor neovascularisation. Perfusion changes in tumor microenvironment were studied in a young patient with a high-grade myxoid liposarcoma after isolated limb perfusion with TNF- α and melphalan, using advanced MR imaging. Quantitative and semi-quantitative evaluation of perfusion metrics included $k^{\text{trans}}/f/T2^*$ shift and automatic extraction of enhancement patterns. Strong agreement between different methods is consistent with response to therapy, specifically reduced perfusion (mean k^{trans} shifted from 0.424 to 0.099 mL/g/min, mean f from 33.5 to 7.3%), reduced hypoxia indication (mean $T2^*$ increased from 72 to 82 ms) and prevalence of necrotic areas.

Keywords

Tumor Necrosis Factor- α ; MR imaging/diagnosis; Pattern Recognition; Tumor hypoxia; Cancer imagenomics; Liposarcoma/treatment response

Abbreviations

(TNF- α)	:	Tumor Necrosis Factor Alpha
ILP	:	Isolated limb perfusion
DCE	:	Dynamic Contrast Enhanced
DWI	:	Diffusion Weighted Imaging
IVIM	:	Intravoxel Incoherent Motion
$T2^*r$:	$T2^*$ Relaxometry
BOLD	:	Blood Oxygen Level-Dependent
PK	:	Pharmacokinetic
k^{trans}	:	Transendothelial permeability
dHb	:	Deoxyhemoglobin
IMVD	:	Intratumoral Microvessel Density
FISH	:	Fluorescence In situ Hybridization
PR	:	Pattern Recognition

Introduction

Isolated limb perfusion (ILP) has been used for locally advanced extremity soft tissue sarcoma in order to avoid amputation when wide excision of the tumor is not feasible [1]. Subsequently (marginal) excision of the tumor is performed 6 to 8 weeks after this regional chemotherapy treatment. A drug combination of tumor necrosis factor alpha (TNF- α) and melphalan is usually used. TNF- α is multifunctional cytokine that plays a major role in innate and acquired immunity while its binding to certain receptors leads to hemodynamic and antitumor effects [2]. The administration of TNF- α during ILP inhibits devastating systemic hemodynamic effects and shows a strong synergistic antitumor action with chemotherapeutic agents in sarcoma patients [3]. In the setting of ILP TNF- α has two distinct antitumor properties that may be related to each other: increased uptake of chemotherapeutic drugs such as melphalan into the tumor and selective destruction of tumor neovascularization [2]. In experimental studies TNF- α has led to increased vessel permeability and decreased interstitial pressure as immediate effects after administration [4,5]. These early antivascular effects lead to an up to 6-fold-increased uptake of melphalan

Article Information

DOI: 10.31021/brr.20181101
Article Type: Research Article
Journal Type: Open Access
Volume: 1 **Issue:** 1
Manuscript ID: BRR-1-101
Publisher: Boffin Access Limited

Received Date: 14 March 2018
Accepted Date: 27 March 2018
Published Date: 29 March 2018

*Corresponding author:

Katerina Nikiforaki, CBML

Foundation for Research & Technology
N.Plastira 100, Vasilika Vouton 70013
Heraklion, Crete, Greece
Tel: +30 2810391658
E-mail: nikiforakik@gmail.com

Citation: Nikiforaki K, Manikis GC, Venianaki M, Lagoudaki E, Maris TG, et al. Perfusion and oxygenation changes after isolated limb perfusion with TNF- α in lower limb sarcoma: a case report. Biomed Res Rev. 2018Mar; 1(1):101

Copyright: © 2018 Nikiforaki K, et al. This is an open-access article distributed under the terms of the Creative Commons Attribution 4.0 international License, which permits unrestricted use, distribution, and reproduction in any medium, provided the original author and source are credited.

into the tumor [6]. Late antivascular effects such as tumor vessel disintegration and endothelial apoptosis which may ultimately result in tumor necrosis are best demonstrated in imaging obtained before and after ILP with TNF- α [7].

The evaluation of tumor response to therapy by non-invasively assessing blood supply and oxygen level has been a long-standing endeavor in MR imaging (MRI). To this end clinically relevant perfusion biomarkers extracted from Dynamic Contrast Enhanced (DCE) Diffusion Weighted Imaging (DWI) and T2* relaxometry (T2*r) are indicative of various pathophysiological properties of tissue vascularity [8,9].

Specifically DCE MRI evaluates the temporal pattern of enhancement from multiple dynamic acquisitions of high temporal resolution. A recent semi-quantitative analysis framework relies on a pattern recognition (PR) method namely BU-NMF [10] which extracts automatically the principal enhancement patterns that describe DCE data and assigns a certain enhancement profile to each image pixel. These patterns can be labeled as necrotic hypoxic and well-perfused and were associated with the three most common enhancement patterns found in tumors [11] which are described by steady and subtle enhancement (Type 1) by delayed enhancement and some wash-out (Type 2) and by rapid enhancement and wash-out (Type 3). Additionally quantitative analysis based on pharmacokinetic (PK) models [12] provides estimates of transfer rates of the contrast agent from plasma to tissue (transendothelial permeability- k^{trans}).

However the DCE is not the only MRI method providing metrics indicative of vascularity. Intravoxel incoherent motion (IVIM) model of DWI may separate microcirculatory from thermal diffusion effects and can be used to study microcirculatory blood flow properties by estimating the microperfusion fraction f [13] i.e. the fraction of DWI signal arising from incoherent blood flow motion.

A third MRI method related to blood supply is the Blood Oxygen Level-Dependent (BOLD) which indirectly measures the total amount of deoxyhemoglobin (dHb) levels in a voxel. Conceptually the paramagnetic nature of deoxyhemoglobin as opposed to oxyhemoglobin accelerates T2* relaxation shortening thus T2* constants of tissue around the blood vessels. Importantly dHb levels depend on a number of concurrent phenomena such as blood flow blood oxygenation vasculature hemoglobin levels etc. [14] Because of the complex interplay between blood supply and oxygen extraction changes in oxygen delivery (blood flow) are not directly related to changes of oxygen consumption and dHb changes do not always match the expected action of the vascular stimulus. T2*r can provide information regarding tumor microenvironment as it reflects tissue oxygen bioavailability. Larger T2* tissue constants as a result of lower dHb concentration may indicate lower blood flow lower tissue oxygenation deficient vascular network etc. and is consistent with tumor response to therapy [9].

Although based on different grounds all three techniques have been widely used for tumor characterization. To our knowledge MRI analysis of TNF induced perfusion have only been studied in animals [15] and have shown changes in endothelial permeability after therapy as measured by perfusion biomarkers. This case study shows the vascularity changes in a lower limb sarcoma after ILP with TNF- α based on quantitative and semi-quantitative MRI methods.

Patient History

A 40-year-old patient was referred for MRI scan of the left foot. Six months prior to imaging he had suffered from local pain during walking and had noticed a gradually growing tumor at its dorsolateral site. X-Ray showed a soft tissue mass between the 4th and the 5th metatarsal bones of the right left foot with bone remodeling and deformity (Figure 1). The mass was painless and slowly growing. Advanced MRI was performed before any biopsy. Since an ultrasound-guided core needle biopsy was inconclusive an open biopsy from the dorsal site of the soft tissue tumor was performed. At histological examination of the macroscopically grey to white color tissue with a myxoid-fleshy consistency the lesion presented a subtle multinodular conformation exhibited areas of variable cellular density with

enhancement of cellularity at the periphery and was composed of bland fusiform or round cells suspended individually in a myxoid matrix with a prominent network of arborizing thin-walled capillary vessels often in a “chicken-footprint” configuration (Figure 2). Pools of extracellular mucin with cellular condensation at the rim were focally present. Mitotic figures were absent and lipoblasts were not identified. Immunohistochemical staining was positive for Vimentin only. Based on rearrangement of DDIT-3 gene which was detected using Fluorescence in Situ Hybridization (FISH) the histopathological diagnosis of high grade myxoid liposarcoma was made.

CT of the lungs revealed small nodular lesions which were considered negative for metastatic disease at the following PET-CT.

In order to avoid amputative surgery the patient underwent ILP from the popliteal vessels with 1 mg TNF- α (administered at time 0') and 65 mg (10 mg/L limb volume administered at time 30') melphalan for a total of 90 minutes. The postoperative course was uneventful and gradual reduction and softening of the tumor were



Figure 1: Magnified oblique view of the left foot, shows a soft tissue mass (asterisk) with displacement and remodelling of the 4th metatarsal (arrow)

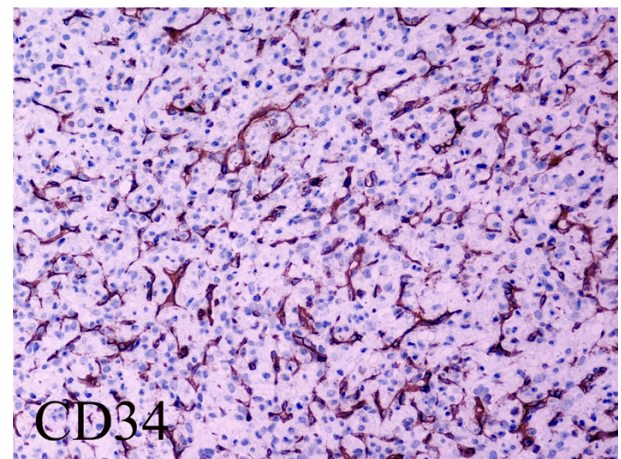


Figure 2: CD34 stain highlights the thin-walled mostly arborizing vasculature (magnification X200)

observed. Two months after ILP and before the planned resection of the tumor MRI demonstrated reduction of the tumor size (Figure 3) whereas advanced MRI was performed for research purposes (Figure 4). A new CT of the lungs demonstrated the presence of multiple lung metastases. Since the patient was asymptomatic the planned resection of the tumor was abandoned and systemic chemotherapy was initiated.

Results

Baseline perfusion study showed strong enhancement (Figure 3a) and further post processing with in-house built software [16,17] evaluated high k^{trans} (mean 0.424 mL/g/min) (Figure 4a) and f values (mean 33.5%) indicating functional vessel network to the neoplasm. The semi-quantitative PR results show that before therapy there is prevalence of the hypoxic enhancement pattern i.e. 59.02% (Figures. 5a, 6). T2* relaxometry showed a mean value for the 3D tumor ROI of 72 ms.

MRI findings before therapy were correlated with immunohistochemistry results (CD34) regarding intratumoral

microvessel density (iMVD). The CD34-stained neoplastic vasculature consisted mostly in fine arborizing vessels with diameter greater than 06 mm and newly formed vessels of one to three endothelial cells. Vessel rich “hot spots” areas were located in the tumor periphery and interestingly correlated closely with the areas having the highest tumor cell proliferation activity (Figure 2). Two methods were used to assess iMVD: a) microvessel counting [18] and b) the relative microvessel area estimate (‘Chalkley count’) [19]. The absolute number of the vessel count obtained in the three fields x200 was 290 282 and 264 respectively resulting in a mean of 280.3 vessels. Chalkley grid score of each hot spot was 14 18 and 16 respectively resulting in a mean Chalkley count of 16.

Visualizing Response to Therapy

Since follow up MRI was performed two months after therapy this study focused on the late vascularity changes such as tumor vessel disintegration and endothelial apoptosis. Identical protocol showed minimal foci of enhancement and reduced number of pixels (873 before vs 618 pixels assigned as tumor after therapy counted in 128x128 DWI images) in the ROI volume (Figure 3b). The semi-

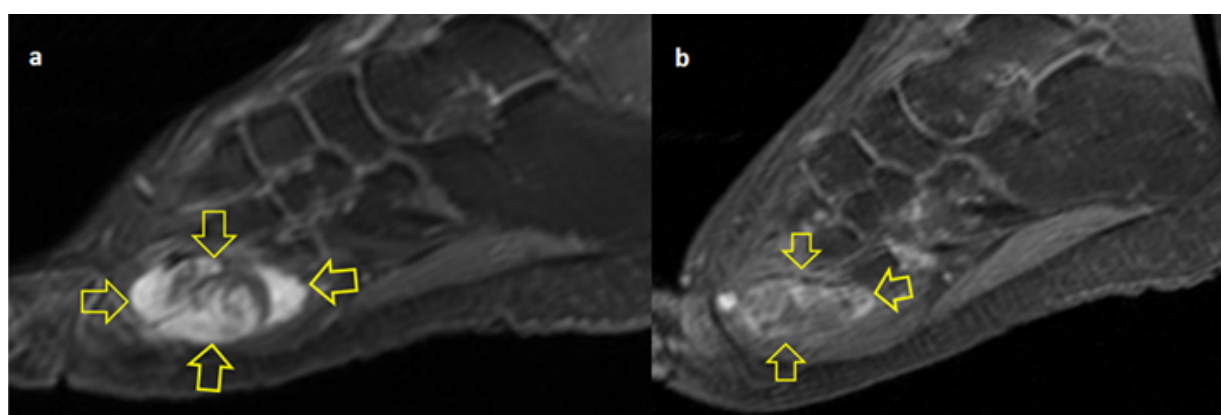


Figure 3: Baseline and follow-up MR imaging

Fat suppressed contrast enhanced sagittal T1-w MR image a) before TNF therapy and b) after TNF therapy, showing the soft tissue mass with intense and in homogenous enhancement (arrows in a) and response to treatment (arrows in b) with regard to both the size of the lesion and the degree of enhancement.

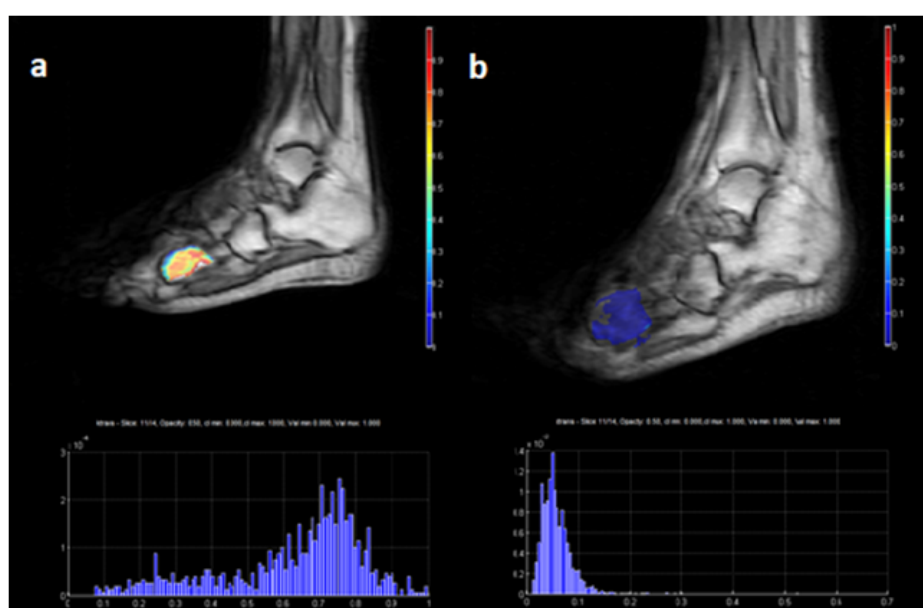


Figure 4: Screenshot from in-house built software platform for DCE longitudinal analysis [16]

Pixel-based parametric (k^{trans}) maps and corresponding histograms from a single slice of the tumor a) before and b) after TNF therapy

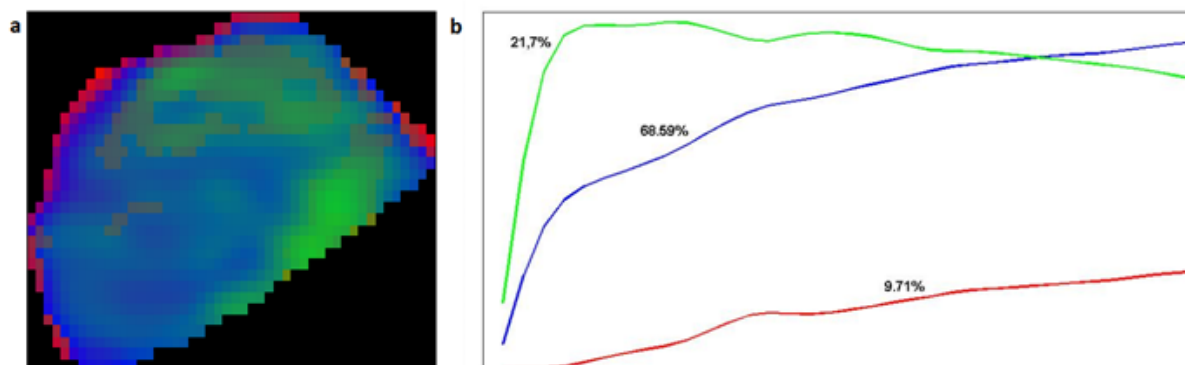


Figure 5: Semi-quantitative results before TNF therapy

a) classification of a single slice of the tumor with the different enhancement patterns, i.e. well-perfused (green), hypoxic (blue) and necrotic (red), identified using pattern recognition techniques

b) plots of the three patterns and corresponding percentage contribution of each one to the whole tumor. The hypoxic pattern (blue) is the principal pattern before TNF therapy

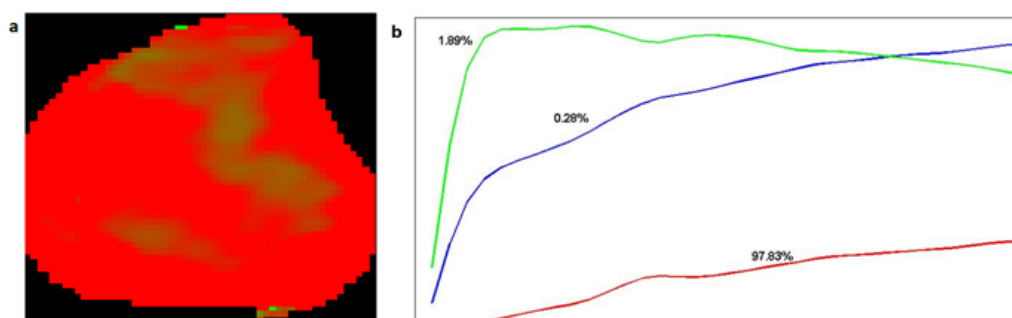


Figure 6: Semi-quantitative results after TNF therapy

a) classification of a single slice of the tumor with the different enhancement patterns, i.e. well-perfused (green), hypoxic (blue) and necrotic (red), identified using pattern recognition techniques and b) plots of the three patterns and corresponding percentage contribution of each one to the whole tumor. The necrotic pattern is dominant after TNF therapy.

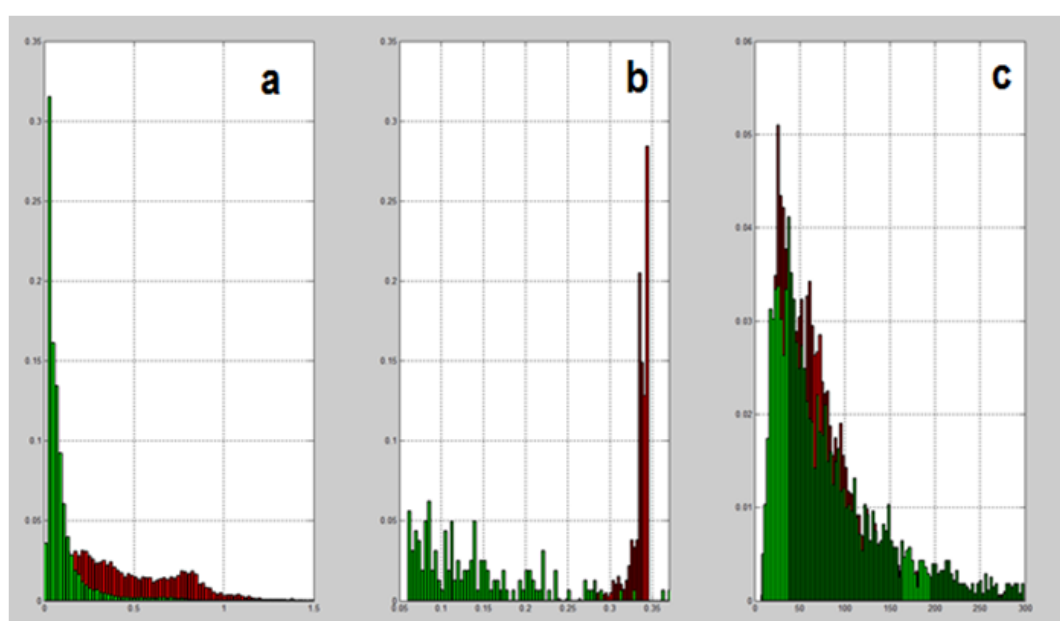


Figure 7: Pixel based histogram analysis before (red) and after (green) TNF therapy from 3-dimensional tumor ROI. a) k^{trans} (mL/g/min), b) f (*100%), c) $T2^*$ (ms).

quantitative approach showed that after therapy the necrotic enhancement pattern is dominant representing a percentage of 97% of image pixels (Figures. 5b,6). All measured k^{trans} metrics [16] show remarkably reduced perfusion in the whole tumor volume (mean was reduced from 0.424 to 0.099 mL/g/min median from 0.349 to 0.06 mL/g/min and 95th percentile from 0.948 to 0.326 mL/g/min) (Figures 4b,7a) strongly indicating severe impairment of the vessel network. Reduced blood flow was also confirmed by decrease of the f metric (mean was reduced from 33.5 to 7.3% median from 33.8 to 5% and 95th percentile from 34.6 to 20.1%) (Figure 7b) [17]. However perfusion changes alone do not suffice to indicate areas of deprived oxygen supply which are important for patient management and assessment of response to therapy. To this end T2* relaxometry was additionally performed. In particular T2* relaxation became slower after therapy (mean was increased from 72 to 82ms median from 61 to 62ms and 95th percentile from 164 to 214ms) implying decreased levels of deoxyhemoglobin (Figure 7c). This finding is in accordance with the aforementioned findings derived from both DCE-MRI and DW-MRI.

Discussion

Quantitative MRI is a powerful tool to assess changes in tumor microenvironment after therapeutic interventions. Although there is no absolute threshold to characterize tumor proliferation hypoxia or necrosis relative changes of perfusion metrics are indicative of changes in vascular permeability oxygen consumption and vascularity and are therefore often used to assess response after therapy. Three-dimensional ROI histogram analysis permits to analyze the whole tumor volume without the need for spatial co-registration between different time points. Mean value shifts in all biomarkers (k^{trans} f T2*) stemming from different methods (DCE DWI T2* respectively) are in accordance with the change of the characteristic dominant perfusion curve of the tumor volume supporting the hypothesis of response to therapy. All metrics compose a complete multifaceted analysis which supports satisfactorily the radiological interpretation.

Conclusion

To conclude this study enabled us to obtain an objective evaluation of the non-invasive assessment of blood supply and oxygen delivery post TNF- α therapy using a combination of DCE DWI and T2* MRI related biomarkers. To our knowledge no study combining more than one perfusion monitoring techniques was found in the recent and older literature in animal or patient population.

References

- Jakob J, Hohenberger P. Role of isolated limb perfusion with recombinant human tumor necrosis factor α and melphalan in locally advanced extremity soft tissue sarcoma. *Cancer*. 2016 May;22(17):2624-2632.
- Locksley RM, Killeen N, Lenardo MJ. The TNF and TNF receptor superfamilies: Integrating mammalian biology. *Cell*. 2001 Feb;104(4):487-501.
- Lienard D, Ewalenko P, Delmotte JJ, Renard N, Lejeune FJ. High-dose recombinant tumor necrosis factor alpha in combination with interferon gamma and melphalan in isolation perfusion of the limbs for melanoma and sarcoma. *J Clin Oncol*. 1992 Jan;10(1):52-60.
- Folli S, Pelegrin A, Chalandon Y, Yao X, Buchegger F, et al. Tumor-Necrosis-Factor Can Enhance Radio-Antibody Uptake in Human Colon-Carcinoma Xenografts by Increasing Vascular-Permeability. *Int J Cancer*. 1993 Mar;53(5):829-836.
- Jahr J, Grande PO. *In vivo* effects of tumor necrosis factor-alpha on capillary permeability and vascular tone in a skeletal muscle. *Acta Anaesthesiol Scand*. 1996 Feb;40(2):256-261.
- de Wilt JH, ten Hagen TL, de Boeck G, van Tiel ST, de Bruijn E a, et al. Tumour necrosis factor alpha increases melphalan concentration in tumour tissue after isolated limb perfusion. *Br J Cancer*. 2000 Mar;82(5):1000-1003.
- Ruegg C, Yilmaz A, Bieler G, Bamat J, Chaubert P, et al. "Evidence for the involvement of endothelial cell integrin $\alpha V\beta 3$ in the disruption of the tumor vasculature induced by TNF and IFN- γ . *Nat Med*. 1998 April;4:408-414.
- Sujana P, Skrok J, Fayad LM. Review of dynamic contrast-enhanced MRI: Technical aspects and applications in the musculoskeletal system. *Journal of Magnetic Resonance Imaging*. 2018 Apr;47(4):875-890.
- Rumley CN, Lee MT, Holloway L, Rai R, Min M, et al. Multiparametric magnetic resonance imaging in mucosal primary head and neck cancer: A prospective imaging biomarker study. *BMC Cancer*. 2017 Jul;17(1):475.
- Venianaki M, Salvetti O, de Bree E, T. Maris, A. Karantanas, et al. Pattern recognition and pharmacokinetic methods on DCE-MRI data for tumor hypoxia mapping in sarcoma. *Multimedia Tools and Application* 2017 Aug;1-23.
- Kuhl CK, Mielcareck P, Klaschik S, Leutner C, Wardelmann E, et al. Dynamic breast MR imaging: are signal intensity time course data useful for differential diagnosis of enhancing lesions? *Radiology*. 1999 Apr;211(1):101-110.
- Tofts PS, Kermode AG. Measurement of the blood-brain barrier permeability and leakage space using dynamic MR imaging. 1. Fundamental concepts. *Magn Reson Med*. 1991 Feb;17(2):357-367.
- Federau C. Intravoxel incoherent motion MRI as a means to measure in vivo perfusion: A review of the evidence. *NMR Biomed*. 2017 Nov;30(11).
- Howe FA, Robinson SP, McIntyre DJO, Stubbs M, Griffiths JR. Issues in flow and oxygenation dependent contrast (FLOOD) imaging of tumours. *NMR Biomed*. 2001 Nov-Dec;14(7-8):497-506.
- Preda A, Wielopolski Pa, Ten Hagen TLM, van Vliet M, Veenland JF, et al. Dynamic contrast-enhanced MRI using macromolecular contrast media for monitoring the response to isolated limb perfusion in experimental soft-tissue sarcomas. *MAGMA*. 2004 Dec;17(3-6):296-302.
- Kontopodis E, Karatzanis I, Sakalis V, Francesca B, Marias K. A DCE-MRI analysis workflow. In: CGI '16: Proceedings of the 33rd Computer Graphics International Conference. 2016:101-104.
- Manikis GC, Nikiforaki K, Papanikolaou N, Marias K. Diffusion Modelling Tool (DMT) for the analysis of Diffusion Weighted Imaging (DWI) Magnetic Resonance Imaging (MRI) data. In: CGI '16: Proceedings of the 33rd Computer Graphics International Conference. 2016:97-100.
- Weidner N, Semple JP, Welch WR, Folkman J. Tumor angiogenesis and metastasis--correlation in invasive breast carcinoma. *N Engl J Med*. 1991 Jan;324:1-8.
- Chalkley HW. Method for the quantitative morphologic analysis of tissues. *J Natl Cancer Inst*. 1943 Aug;4(1):47-53.